

Preparation, characterization, and application of synthesized thiourea formaldehyde-calcium alginate in removal of Reactive Black 5

A.A. El-Bindary, A.F. Shoair, H.A. Kiwaan, and A.R. Hawas

Abstract: Thiourea formaldehyde calcium alginate (TFCA) composite was successfully synthesized and used for removal of Reactive Black 5 (RB5) dye. The synthesized composite was applied and characterized by Fourier transform infrared spectrometer (FTIR) spectra, scanning electron microscope (SEM)/EDS, energy dispersive X-ray analysis (EDX), and X-ray diffraction (XRD). SEM and EDX analyses confirm the homogeneity of the sorbent in term of composition. Batch adsorption experiments were performed to evaluate the adsorption conditions such as pH value, dye concentration, contact time, temperature, and sorbent dose, as well as the ionic strength effect. Experimental data have been modeled by using Langmuir, Freundlich, Dubinin Radushkevich (D-R), and Temkin isotherms. Kinetic adsorption data modeled using PFORE, PSORE, Morris Weber, and Elovich in order to determine thermodynamic parameters (ΔG , ΔH , and ΔS) for the dye adsorbent systems. These data indicated an exothermic spontaneous adsorption process that kinetically followed the pseudo second-order adsorption process and removal of RB5 dye from aqueous solution. The results showed that the maximum adsorption capacity was 0.2 mmol g^{-1} , observed at pH 1 and temperature $25 \text{ }^\circ\text{C}$. Equilibrium adsorption was achieved within 60 min.

Key words: RB5, composite, isotherm, kinetics, thermodynamics.

Résumé : Nous avons synthétisé un composite de résine thiourée-formaldéhyde et d'alginate de calcium (TFCA) et nous l'avons appliqué à l'enlèvement du colorant Reactive Black 5. Nous avons caractérisé le composite synthétisé par spectroscopie infrarouge à transformée de Fourier (FTIR), analyse par microscopie électronique à balayage (MEB)/EDS, spectroscopie à dispersion d'énergie (EDS) et diffraction des rayons X (DRX). Les analyses par MEB et EDS confirment l'homogénéité de la composition du sorbant. Nous avons réalisé des expériences d'adsorption en lots pour évaluer les conditions d'adsorption telles que le pH, la concentration du colorant, le temps de contact, la température et la quantité de sorbant, ainsi que l'effet de force ionique. Nous avons modélisé les données expérimentales à l'aide des isothermes de Langmuir, de Freundlich, de Dubinin Radushkevich (D-R) et de Temkin. Nous avons modélisé les données cinétiques d'adsorption à l'aide des modèles PFORE, PSORE, Morris Weber et Elovich pour déterminer les paramètres thermodynamiques (ΔG , ΔH et ΔS) des systèmes colorant-adsorbant. Ces données indiquent que le processus d'adsorption est spontané et exothermique et qu'il suit une courbe cinétique d'adsorption de pseudo second ordre. Lorsque nous avons appliqué le composite à l'enlèvement du colorant RB5 d'une solution aqueuse, les résultats ont montré que la capacité maximale d'adsorption était de $0,2 \text{ mmol g}^{-1}$ à pH 1 et à température de $25 \text{ }^\circ\text{C}$. L'équilibre d'adsorption a été atteint en 60 minutes. [Traduit par la Rédaction]

Mots-clés : RB5, composite, isotherme, cinétique, thermodynamique.

Introduction

Water pollution is an important environmental problem and a worldwide concern.¹⁻³ Dyes discharged together with industrial textile wastewaters are major organic pollutants, as they are highly visible and undesirable even at low concentrations in water.⁴⁻⁶ More seriously, most organic dyes are toxic, nonbiodegradable, and even teratogenic, carcinogenic, mutagenic, which create serious threats to human health and marine organisms.^{7,8} Dyes are used in large quantities in various industries including textile, healthcare, paint, printing, leather processing, and food processing to colour their products. Hence, the dyes must be efficiently removed from the discharged wastewater to solve the ecological, biological, and industrial problems. Many treatment options for dye removal include chemical, biological, and physical methods. Some of the many physical methods used for dye removal from aqueous solution include adsorption, electrochemical precipitation, ion ex-

change, membrane filtration (ultrafiltration, reverse osmosis) irradiation, and electrokinetic coagulation.^{9,10} Adsorption techniques have been shown to be a feasible option, both technically and economically. The adsorbents with high capacity and high rate play a critical role in the adsorption removal of dye molecules. Many works have been published investigating the removal of dyes from industrial effluents. The present study reports the synthesis and characterization of thiourea formaldehyde calcium alginate (TFCA) and its dye adsorption efficiency of Reactive Black 5 (RB5) dye ions removal by batch technique. TUF resin can be synthesized easily in aqueous solutions by controlling the acidity during the synthesis. The synthesis includes hydroxy methylation and condensation steps. TUF resin has a very complex structure depending on the mole ratio of thiourea to formaldehyde and attains a high surface area and excellent adsorption capacity.¹¹ Alginate is by far the most popular biopolymer for immobilization purposes. Alginate forms sol-gel propagules easily, has

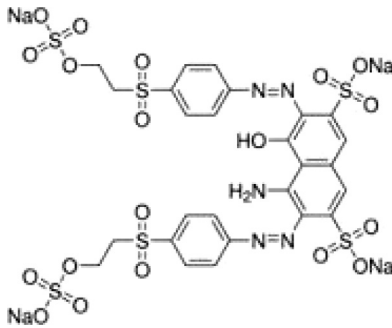
Received 27 January 2018. Accepted 14 August 2018.

A.A. El-Bindary, A.F. Shoair, H.A. Kiwaan, and A.R. Hawas. Chemistry Department, Faculty of Science, Damietta University, Damietta 34517, Egypt.

Corresponding author: A.R. Hawas (email: ahmed_hawas_a_h@yahoo.com).

Copyright remains with the author(s) or their institution(s). Permission for reuse (free in most cases) can be obtained from [RightsLink](https://www.nrcresearchpress.com/permissions).

Table 1. Properties of the adsorbate (RB5) anionic dye.

Parameter	Characteristic
Name	Reactive Black 5
Abbreviation	RB5
Type colour	Anionic
Chemical formula	$C_{26}H_{21}N_5Na_4O_{19}S_6$
Molecular weight (g/mol)	991.82
Wavelength of maximum absorption (nm)	597
Molar extinction coefficient, ϵ_{597} ((mol/L) $^{-1}$ cm $^{-1}$)	34 450
Chemical structure of colour	

good acid stability, and has remarkable dye ion adsorption properties attributed to the presence of carboxylic groups on the surface of the alginate beads;¹² modifications of thiourea-formaldehyde sorption properties by incorporation of sorptive materials such as calcium alginate improve sorption performance of alginate through amine and thio groups of thiourea. To the best of our knowledge, there have been no reports on thiourea-formaldehyde crosslinked alginate resin. Experimental parameters affecting the adsorption process such as pH solution, initial adsorbate concentration, contact time, temperature, adsorbent dosage, and solution ionic strength were studied. The experimental equilibrium adsorption data were analyzed by isotherm and kinetic models. The thermodynamics of the adsorption indicated spontaneous and endothermic nature of the sorption process.

Experimental

Chemicals and reagents

All chemicals were of analytical grade and demineralized water was used for the preparation of all aqueous solutions. Sodium alginate was purchased as alginic acid sodium salt (Fluka Co), acid dye RB5 (Table 1) was obtained from Cromatos SRL, and hydrochloric acid (HCl 35%), sodium hydroxide (NaOH 99.9%), and $CaCl_2$ were supplied by Merck Company (Germany). A stock solution whose concentration was 1×10^{-3} mol/L was used and could be diluted to the required concentration with demineralized water in the experiment. All chemical reagents were analytical grade and used as received.

Physical measurements

To confirm the functionalization of the sorbent thiourea formaldehyde calcium alginate (TFCA) composite, spectroscopic data of the investigated dye were obtained using the following instruments. Fourier transform infrared (FTIR) spectrophotometer spectra (KBr discs, 4000–400 cm^{-1}) were obtained by a Jasco-4100 spectrophotometer. The SEM results of the MSAB sample before and after the adsorption processes were obtained using the JEOL-JSM-6510 LV scanning microscope to observe surface modification. The structure of the synthesized adsorbents was examined by X-ray diffraction measurement (XRD) and was recorded on X-ray diffractometer in the range of diffraction angle $2\theta = 5-80^\circ$. The elemental distribution of TFCA was analyzed using the energy-dispersive X-ray spectroscopy (EDX) and taken on a Leo1430VP micro-

scope with operating voltage of 5 kV. The Brunauer–Emmett–Teller (BET) surface area and Barrett–Joyner–Halenda (BJH) pore volume that form N_2 adsorption–desorption isotherms on MSAB at 77 K measured on a Quantachrome Nova Instruments version 10 were calculated. A UV-vis spectrophotometer (Perkin-Elmer AA800 Model AAS) was employed for absorbance measurements of samples. A HANNA Instruments pH meter (model 211) and Maxturdy 30 (Wisd) instrument were used for pH adjustment and shaking, respectively.

Synthesis of thiourea-formaldehyde encapsulated alginate

Synthesis of the thiourea-formaldehyde polymer

First, 15.2 g (0.2 mol) of thiourea and 40 mL of distilled water were mixed in a 250 mL necked flask equipped with a stirrer and condenser. The flask was heated until thiourea was dissolved. Then, 15 mL of formaldehyde (37% aqueous solution, containing 0.2 mol of formaldehyde) was added to the reaction mixture and the solution pH was adjusted to 3 with 2 mL of acetic acid. The reaction was carried out for 6 h with heating (95 °C) and stirring. The product was washed with dilute NaOH solution, distilled water, and ethanol.

Encapsulated of alginate with thiourea-formaldehyde

Fifty grams of sodium alginate solution (4%, w/v) was mixed with 4 g of thiourea-formaldehyde resin and 48 mL of distilled water. The mixture of alginate and the resin powder was distributed dropwise into a $CaCl_2$ (20 g L^{-1}) stirred solution. The gel beads were kept in the $CaCl_2$ solution for 24 h, for complete gelation. Finally, the produced calcium alginate beads encapsulated with thiourea-formaldehyde resin rinsed with distilled water, ethanol, and acetone and then dried at room temperature.

There were three goals for the modification of thiourea-formaldehyde resin with alginate. First, it was impossible to use the fine particles of thiourea-formaldehyde resin in column systems (head loss and clogging effect). Second, these composite materials take advantage of the sorption properties of both thiourea-formaldehyde resin and alginate. Third, amine and thio groups from thiourea contribute to improved sorption performance of alginate.

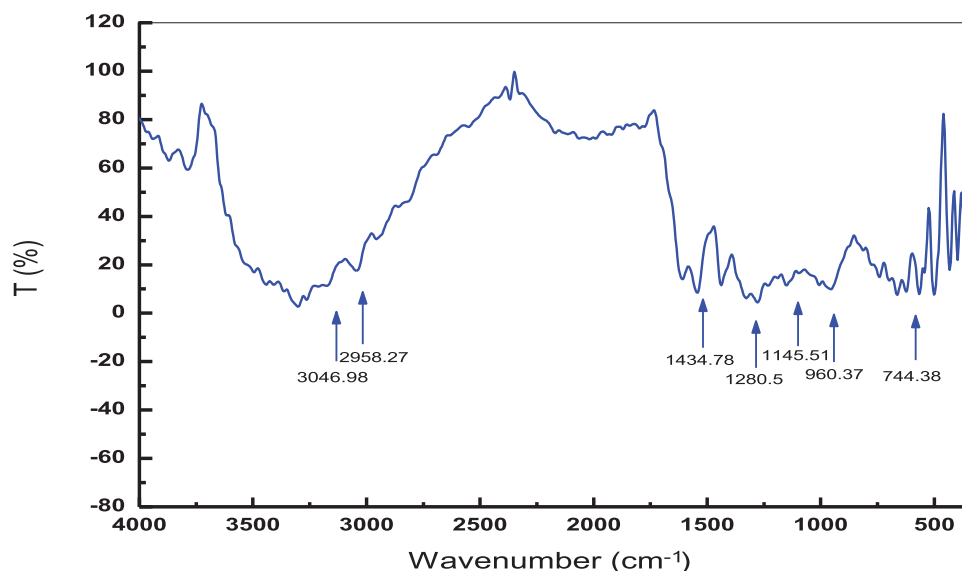
Batch adsorption studies

The adsorption experiments of anionic dye RB5 were carried out in batch equilibrium mode. A 0.02–0.1 g sample of TFCA composite with 25 mL aqueous solution of a $1.2 \times 10^{-5} - 5 \times 10^{-5}$ mol/L RB5 solution at various pH values (1–9) reached for 120 min was adjusted by adding a small amount of HCl or NaOH solution (0.01–0.1 mol/L) using a pH meter. Samples were collected and filtrated through a Whatman (number 40) filter paper, and the filtrates were subjected to quantitative analyses. The equilibrium concentration of each solution was determined at the wavelength of UV maximum (λ_{max}) at 597 nm using a Perkin-Elmer AA800 spectrophotometer model AAS. Dye adsorption experiments were also accomplished to obtain isotherms at various temperatures (20–40 °C) and at a range of dye concentrations ($1.2 \times 10^{-5} - 5 \times 10^{-5}$ mol/L) for 90 min by using a shaker water bath. These experiments were carried out with different ionic strength, dye concentration, and adsorbent dosage.

Results and discussion

Characterization of adsorbents

The various constituents of TFCA per chemical and analytical technique are applied and characterized with further analysis. The SEM photographs revealed the absorptive nature of adsorbent. The presence of TFCA was examined by XRD measurement. The elemental distribution of TFCA was analyzed using EDX spectroscopy. N_2 adsorption/desorption isotherms on TFCA was mea-

Fig. 1. FTIR spectrum of the TFCA adsorbent. [Colour online.]

sured on a Quantachrome Nova Instruments version 10, from which the BET surface area and BJH pore volume were calculated.

Infrared spectrometry

The FTIR spectra of TFCA particles wave number range 4000–400 cm^{-1} (Fig. 1) showed that the broad band's appearance in the range of 3500–3200 cm^{-1} can be attributed to the hydroxyl group (O–H stretching vibrations) of calcium alginate. The symmetric and asymmetric aliphatic C–H stretching bands were observed at 3046.98 and 2958.27 cm^{-1} , respectively. The bands at 1608.34 and 1546.63 cm^{-1} were attributed to the asymmetric and symmetric stretching vibrations of carboxylate group of alginates, respectively. The bands at 1434.78 and 1280.5 cm^{-1} were attributed to the C–O stretching vibration of pyranosyl ring and the C–O stretching with contributions from C–C–H and C–O–H deformations, respectively.¹³ The peak at 1145.51 cm^{-1} for C–O–C stretching was also seen with TF resin. The band at 960.37 cm^{-1} was for the thiourea functional group N–C–S stretching and the band at 744.38 cm^{-1} was for C–S stretching.¹⁴ Thus, we inferred that thiourea-formaldehyde was encapsulated with alginate resin. The spectra of dye loaded (TFCA) sorbent have very similar FTIR profiles as the same bands are appearing on all spectra, only small differences are observed, namely a small shift in some of these bands.

Scanning electron microscope (SEM)

SEM has been a primary tool for characterizing the surface morphology and fundamental physical properties of the adsorbent surface. It is useful for determining the particle shape, porosity, and appropriate size distribution of the adsorbent. Scanning electron micrographs of raw TFCA and adsorbed (RB5) TFCA are shown in Figs. 2a and 2b, respectively. Figure 2a shows a granular material of CaCO_3 coating on TFCA; the considerable numbers of pores provide a good possibility for dye to be trapped and adsorbed into these pores. The SEM picture of TFCA adsorbed with tested dye (RB5) shows very distinguished dark spots (Fig. 2b) that can be taken as a sign for effective adsorption of RB5 dye molecules in the cavities and pores of this adsorbent.

XRD analysis

XRD analysis (Fig. 3) was used for characterizing the crystalline structure of the material, which is induced by the magnetite core. The XRD pattern shows that a limited number of peaks, which are characteristic of iron oxides, may be identified. The large fraction of polymer may contribute to the explanation of the poor resolu-

tion of the XRD pattern. The peaks characteristics of TFCA^{15,16} are usually identified at indices: 16.8 (98), 21.94 (158), 43.96 (70), 64.3 (54), and 77.42 (70).

EDX spectroscopy analysis

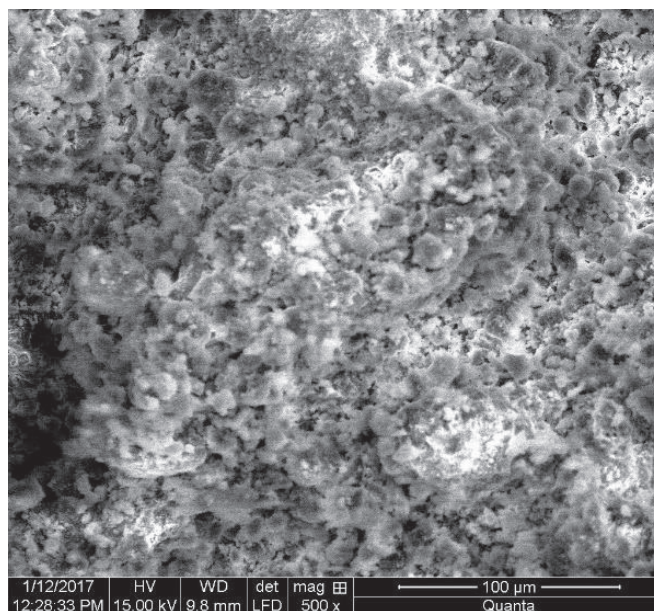
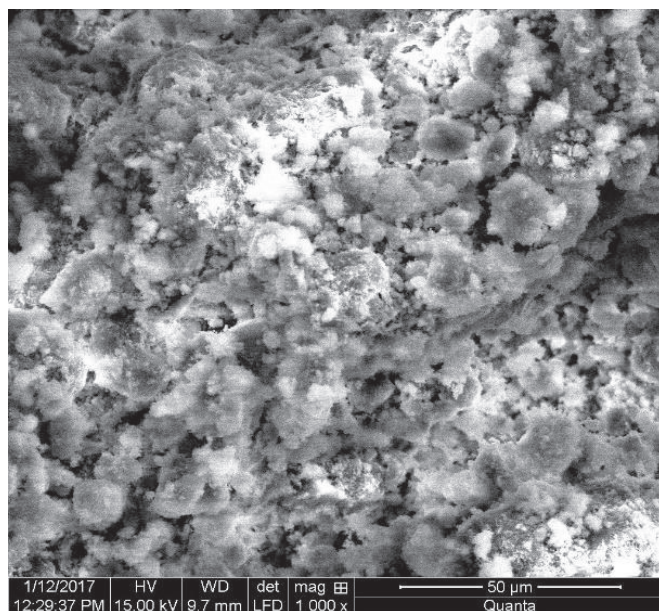
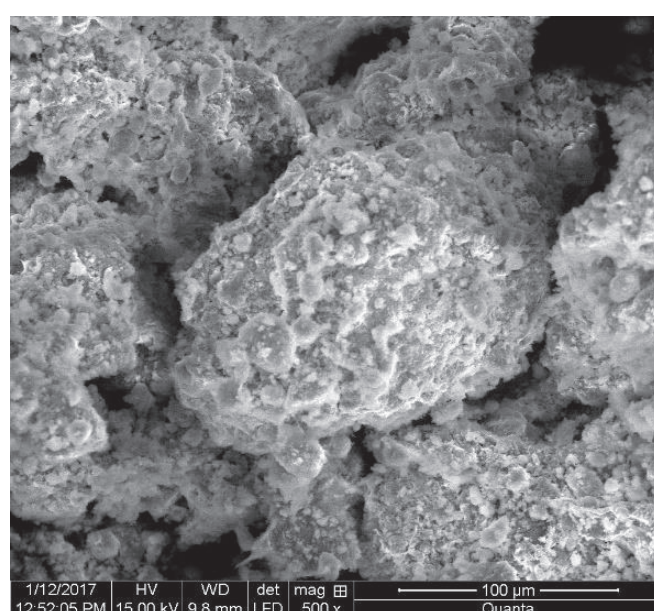
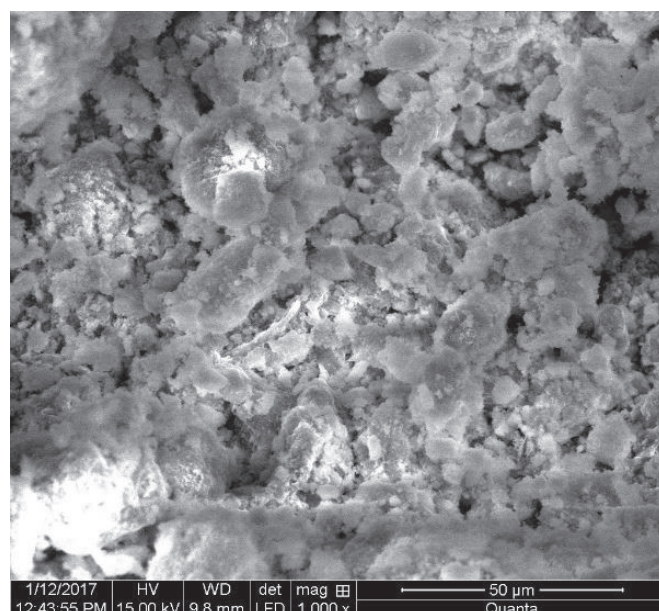
From the EDX analysis of the corresponding surface (Fig. 4), it can be seen that the boundary film was composed of TFCA. EDX analysis of free TFCA: element (Wt %): C 28.71; N 21.40; O 9.92; S 37.40; Ca 2.56. Element (At %): C 41.43; N 26.49; O 10.75; S 20.22; Ca 1.11. Element (K-Ratio): C 0.0309; N 0.0206; O 0.0105; S 0.3523; Ca 0.0196.¹⁷

BJH pore volume and BET surface area

The N_2 adsorption–desorption isotherm determined at 77 K on the prepared sample (TFCA) is illustrated in Fig. 5. The specific surface area is estimated by application of the BET equation in its normal range of applicability with a value of 16.20 \AA for the cross-section area of N_2 molecule. The total pore volume, taken at $P/P_0 = 0.9477$, and the pore size distribution is estimated by the BJH method. The adsorption isotherm of the sample is classified as type (II) with H4 hysteresis loop classified by IUPAC that extending down to $[P/P_0] = 0.38$; this deep hysteresis loop arises from aggregates (assemblage of particles that are loosely coherent) of plate-like form giving rise to slit-shaped pores.¹⁸ The wide hysteresis loop reveals the remarkable mesoporous structure of the prepared sample. The surface area $A_{\text{BET}} = 55.134 \text{ m}^2/\text{g}$, the total pore volume = 0.093 cm^3/g , and the average pore radius = 33.77 \AA , which confirms the mesoporosity of the prepared sample. The narrow pore size distribution reveals the homogeneity of the pore size through the sample matrix.

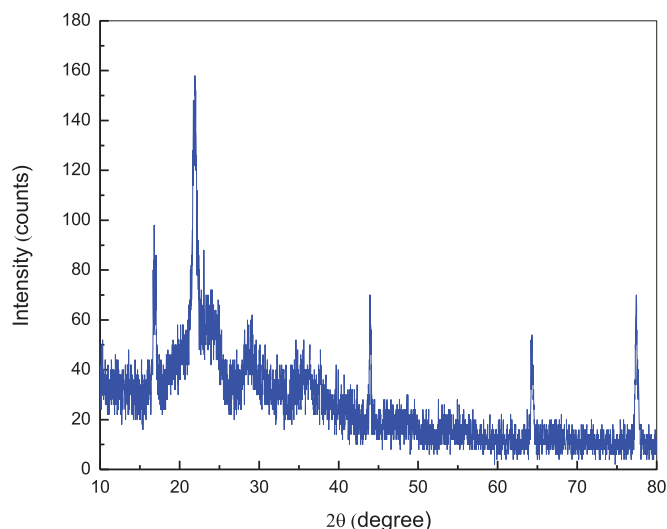
Determination of point of zero charge

The point of zero charge (pH_{PZC}) was determined by solid addition method.¹⁹ A series of 0.1 mol/L KNO_3 solutions (25 mL) were prepared and their pH values (pH_0) were adjusted in the range of 1–12 by addition of 0.01–0.1 mol/L HCl and NaOH. To each solution, 0.1 g of TFCA was added and the suspensions were agitated in an orbital shaker at 200 r/min. The final pH values of the supernatant were determined (pH_f) after 48 h. The difference between initial (pH_0) and final (pH_f) values ($\Delta\text{pH} = \text{pH}_0 - \text{pH}_f$) (y axis) was plotted against the initial pH_0 (x axis). The intersection of resulting curve yielded the pH_{PZC} where $\Delta\text{pH} = \text{zero}$.

Fig. 2. Scanning electron micrographs of (a) unloaded TFCA and (b) RB5-loaded TFCA.**a****b****Batch adsorption analysis****Effect of pH**

pH definitely affects the adsorption of the dye. To determine the adsorption behavior of the dye,²⁰ tests were carried out at predetermined experimental conditions taking the initial dye concentration as 1×10^{-4} mol/L, temperature as 25 °C, and adsorbent dosage as 0.02 g. Solutions (0.01 and 0.1 mol/L) of NaOH and HCl were employed to adjust the pH of the test solutions. In the case of adsorption of RB5 on TFCA, a pH range of 1–9 was selected. The TFCA composite has proven to be an effective adsorbent for the removal of acid dye (RB5) via adsorption from aqueous solution at

pH 1 (Fig. 6). It shows that the adsorption capacity of acid dye RB5 onto TFCA composite increases significantly with decreasing pH, which is due to neutralization of the positive charge at the surface of the adsorbents by the negatively charged dye molecule. The maximum removal of RB5 for a contact time of 90 min was carried out at pH 1. At strongly acidic pH values, a significantly high electrostatic attraction exists between the positively charged surface of the adsorbent and the negatively charged dye molecules ($-\text{SO}_3\text{Na}$).²¹ As the pH of the adsorption system increases, the number of negatively charged sites increases and the number of positively charged sites decreases. A negatively charged surface site on

Fig. 3. Powder XRD pattern of TFCA particles. [Colour online.]

the adsorbent does not favor the adsorption of dye anions, due to the electrostatic repulsion. Moreover, the lower adsorption of RB5 at alkaline pH is due to the presence of excess hydroxyl ions competing with the dye anions for the adsorption sites.²² Basic conditions favor adsorption of dye; thus pH 1 was considered as the optimum pH for the adsorption of the dye.

Effect of adsorbate concentration

The removal of RB5 dye by adsorption on the adsorbent (TFCA) composite was shown to increase with time and attained a maximum value at about 60 min, and thereafter, it remained almost constant (Fig. 7). Adsorption experiment for the dye RB5 were carried out by selecting a concentration range of 1.2×10^{-5} to 5×10^{-5} mol/L with an adsorbent dosage of 0.02 g at 25 °C and pH 1. The amount of removed dyes decreased. It was clear that the removal of the dye was dependent on the initial concentration of the dye, because the decrease in the initial dye concentration increased the amount of dye adsorbed. This is very clear because, for a fixed adsorbent dose, the number of active adsorption sites to accommodate adsorbate ions remains unchanged; however, with increasing adsorbate concentration, the adsorbate ions to be accommodated increase and hence the percentage of adsorption goes down.

Effect of contact time

The amount of the dye adsorbed at definite intervals of time at 25 °C was monitored for a fixed amount of TFCA at a particular concentration. Figure 8 indicates that with the increase in time, the adsorption rate of the dye over adsorbent increases with time and attained a maximum value at about 60 min. Thereafter, the amount of time required to bring complete saturation of the active sites of adsorbent remained almost constant at 120 min.

Effect of temperature

Temperature dependence of the adsorption process is associated with several thermodynamic parameters. The plot of amount of adsorbate per amount of adsorbent of adsorption as a function of temperature (Fig. 9) shows a small increasing trend with a rise in temperature from 25 °C to about 45 °C. Equilibrium capacity can be changed by temperature of the adsorbent for a particular adsorbate. In our case, the experimental data obtained at pH 1, adsorbent dosage of 0.02 g, and initial concentration of 3×10^{-5} mol/L show no change in the adsorption capacity at temperatures ranging from 25 to 45 °C. The increase in adsorption with increasing temperature also indicates the endothermic nature of the dye adsorption over adsorbent.

Effect of adsorbent dosage

The study of the effect of amount of the adsorbents was necessary to observe the minimum possible amount that shows maximum adsorption. The amount of the adsorbent varied from 0.02 to 0.1 g. In this experiment, the adsorptive ability of the adsorbent at a definite concentration of 3×10^{-5} mol/L dye solution at pH 1 at 25 °C was considered (Fig. 10). Adsorption of dyes as a function of the TFCA composite dosage shows that the uptake of dye per gram of adsorbent increases with increasing adsorbent dosage from 0.02 to 0.06 g. This is because a higher dose of adsorbent led to increased surface area and more adsorption sites are available causing higher removal of the dyes.²³ Further increase in adsorbent dose did not cause any significant increase in percent removal of dyes. This was due to the concentration of dyes reached at equilibrium status between solid and solution phase.

Effect of ionic strength (addition of NaCl)

The effect of chloride ions on RB5 removal was examined by addition of increasing concentrations of NaCl (Fig. 11). For the studied adsorbents, increasing the amount of NaCl slightly decreases the sorption capacity; the sorption capacity decreases by 20% when the NaCl concentration reaches 20 g L⁻¹. This is probably due to the competitor effect of chloride anions against RB5 anions for interaction with adsorption sites. It is noteworthy that even when the NaCl concentration reaches 40 g L⁻¹, the reduction in the adsorption capacity decreases by 1.5%; this indicates that even under these drastic conditions a high adsorption capacity is maintained.

Adsorption studies

Adsorption isotherms

The main factors that play key roles for the dye-adsorbent interactions are charge and structure of dye, adsorbent surface properties, hydrophobic and hydrophilic nature, hydrogen bonding, electrostatic interaction, steric effect, and van der Waals forces.²⁴ Equilibrium studies that give the capacity of the adsorbent and adsorbate are described by adsorption isotherms, which are usually the ratio between the quantity adsorbed and the quantity that remained in solution at equilibrium at a fixed temperature.²⁵ The equilibrium relationships between adsorbent (TFCA) and adsorbate (RB5) are best explained by sorption isotherms.

The present investigation deals with the applicability of Langmuir, Freundlich, Dubinin-Radushkevich (D-R), and Temkin adsorption isothermal models to the experimental data.

Langmuir isotherm

The Langmuir adsorption, which is the monolayer adsorption, depends on the assumption that the intermolecular forces decrease rapidly with distance and, consequently, predicts the existence of monolayer coverage of the adsorbate at the outer surface of the adsorbent. The isotherm equation further assumes that adsorption occurs at specific homogeneous sites within the adsorbent. It then assumes that once a dye molecule occupies a site, no further adsorption can take place at that site. Furthermore, the Langmuir equation makes the assumption of a structurally homogeneous adsorbent, where all sorption sites are identical and energetically equivalent. Theoretically, the sorbent has a finite capacity for the sorbate. Therefore, a saturation value is reached beyond which no further sorption can occur. The saturated or monolayer capacity can be represented as the known linear form of Langmuir equation^{26,27}

$$(1) \quad \frac{C_e}{q_e} = \frac{1}{q_{\max} K_l} + \frac{C_e}{q_{\max}}$$

where C_e is the equilibrium dye concentration in solution (mol L⁻¹), q_e is the equilibrium dye concentration in the adsorbent (mmol g⁻¹),

Fig. 4. EDX spectroscopy of TFCA.

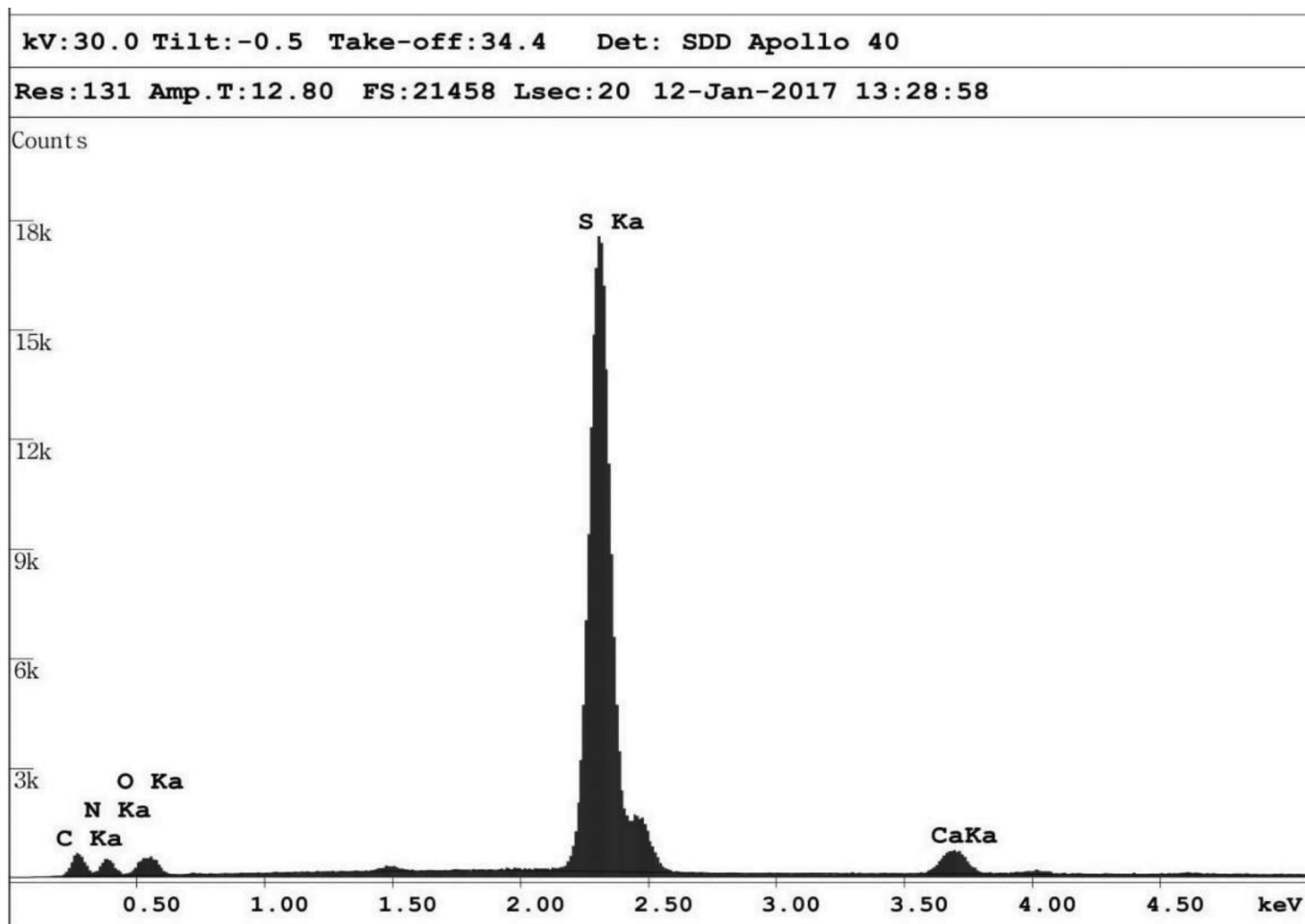
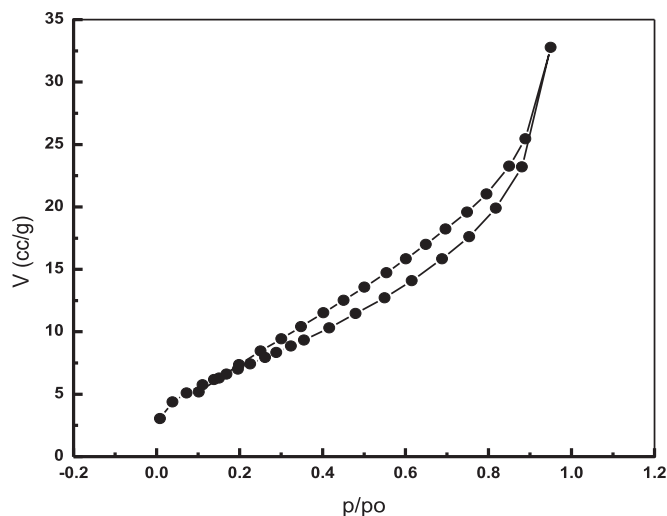


Fig. 5. Pore volume and surface area for TFCA.



q_{\max} is the monolayer capacity of the adsorbent (mmol g^{-1}), and K_L is the Langmuir adsorption constant (L mol^{-1}). Therefore, a plot of C_e/q_e vs. C_e (Fig. 12a) gives a straight line of slope $1/q_{\max}$ and the intercept $1/(q_{\max}K_L)$. The Langmuir equation is applicable to homogeneous sorption, where the sorption of each sorbate molecule onto the surface is equal to sorption activation energy, with the help of which Langmuir constants can be calculated (Table 2).

Freundlich isotherm

The Freundlich isotherm is a result of the assumptions that the adsorption occurs on a heterogeneous surface and that non-uniform distribution of the heat of adsorption over the adsorbent surface takes place, characterized by the heterogeneity factor $1/n$. This isotherm describes reversible adsorption and is not restricted to the formation of the monolayer.

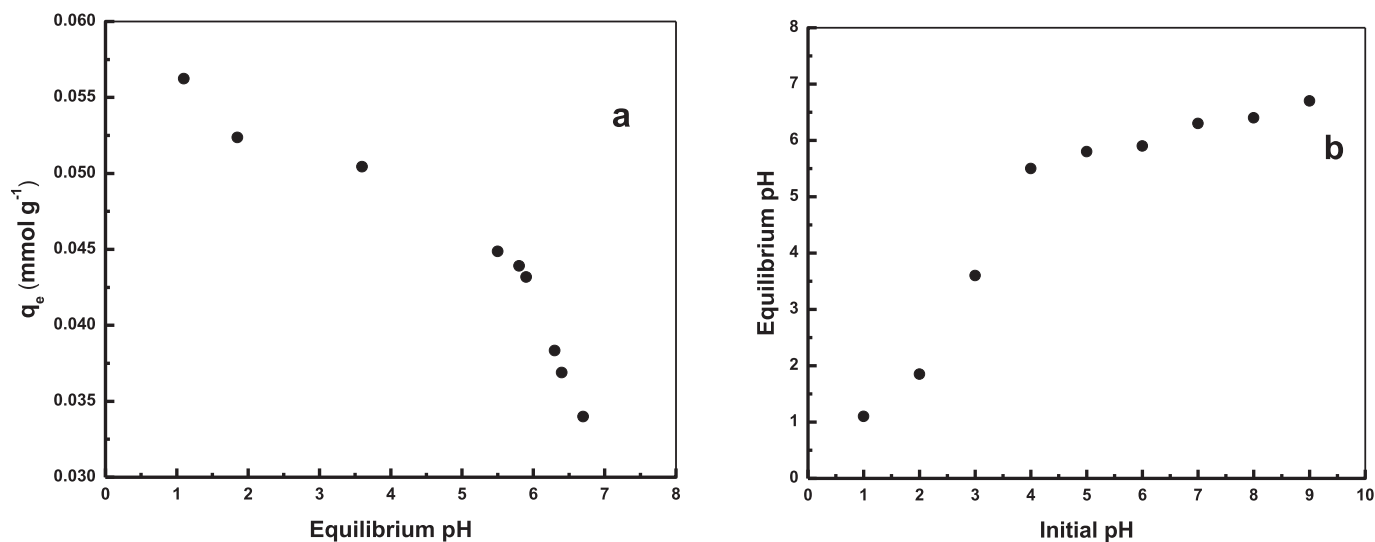
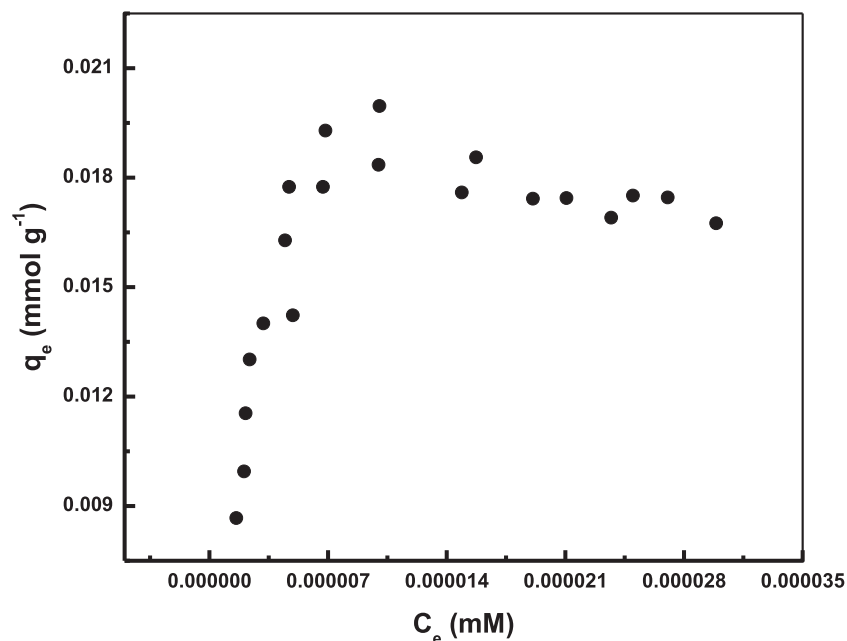
$$(2) \quad q_e = K_F C_e^{1/n}$$

where q_e is the equilibrium dye concentration on adsorbent (mmol g^{-1}), C_e is the equilibrium dye concentration in solution (mol L^{-1}), K_F is the Freundlich constant (L g^{-1}), and $1/n$ is the heterogeneity factor. A linear form of the Freundlich expression can be obtained by taking anti logarithms of the equation:

$$(3) \quad \ln q_e = \ln K_F + \frac{1}{n} \ln C_e$$

Therefore, a plot of $\log q_e$ vs. $\log C_e$ for the adsorption of RB5 onto TFCA composite was employed to generate the intercept value of K_F and the slope of $1/n$. The graphical presentation for the Freundlich isotherm for the adsorbent, as well as its R^2 values, is given in Fig. 12b. High R^2 values of the straight lines obtained confirm the validity of Langmuir adsorption isotherm for the adsorbent. The Freundlich constants for the adsorbent are presented in Table 2.

The Langmuir and Freundlich parameters for the adsorption of RB5 are listed in Table 2. It is evident from these data that the

Fig. 6. pH effect on adsorption of RB5 using the adsorbent. Temperature = 25 ± 1 °C; $C_0 = 1 \times 10^{-4}$ mol/L.**Fig. 7.** Adsorption isotherms onto the adsorbent. pH 1; temperature, 25 ± 1 °C.

surface of the TFCA composite is mostly made up of heterogeneous adsorption patches.

On comparing the regression coefficients obtained for Langmuir and Freundlich, it can be very well predicted that the Langmuir isotherm is more favored by the adsorption process. The data presented above clearly show that the Langmuir adsorption isotherm graphs (Fig. 12a) are better fit than the Freundlich adsorption isotherm graphs (Fig. 12b). This indicates that a monolayer adsorption process, taking place in the present case, is more favorable than multilayer formation of the adsorbate.

The dimensionless parameter of equilibrium, separation factor “ r ” suggested by Mittal et al.²⁸ can be calculated as follows:

$$(4) \quad r_L = \frac{1}{1 + K_L C_0}$$

where C_0 is the initial concentration, and K_L signifies the Langmuir constant. There are four probabilities for the value of r : (i) for

favorable adsorption, $0 < r < 1$, (ii) for unfavorable adsorption, $r > 1$, (iii) for linear adsorption, $r = 1$, and (iv) for irreversible adsorption, $r = 0$. The obtained values of separation factor are 0.168, 0.158, 0.148, and 0.14 for TFCA at a temperature of 25 °C, clearly indicating the favorability of the adsorption process.

The correlation coefficients for Langmuir (R_L^2) and Freundlich (R_F^2) values are provided in Table 2. One of the Freundlich constants, K_F , indicates the adsorption capacity of the adsorbent. The other Freundlich constant, n , is a measure of the deviation from linearity of the adsorption. If a value for n is equal to unity, then the adsorption is linear. If a value for n is below unity, then this implies that the adsorption process is chemical. Alternatively, if a value for n is above unity, then adsorption is a physical process.²⁹ The highest value of n at equilibrium is 2.62 (Table 2), which represents favorable adsorption, and therefore, this would seem to suggest that the adsorption is physical, which is preferred when the adsorption bond becomes weak³⁰ and conducted with van der Waals forces rather than chemical adsorption.

Fig. 8. Effect of contact time.

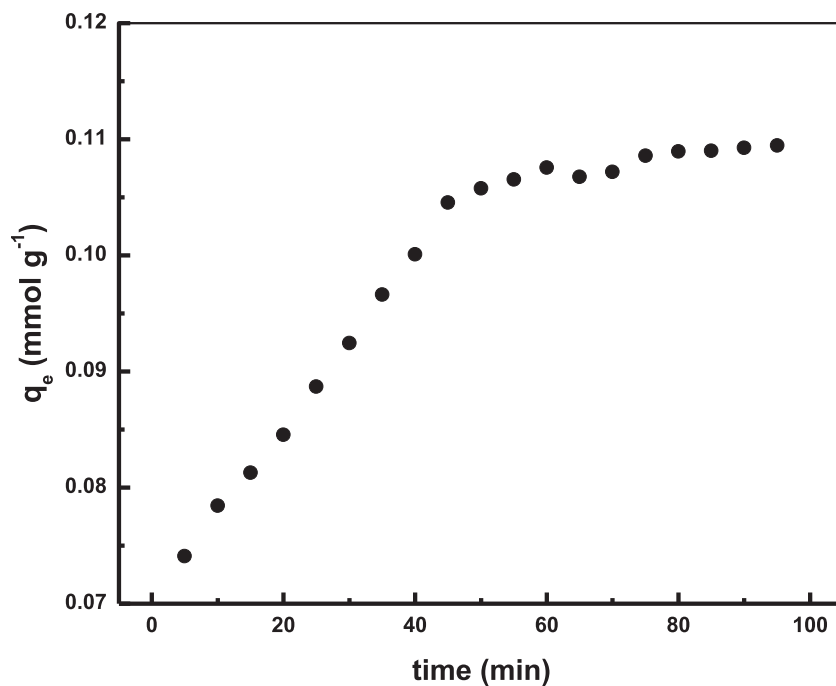
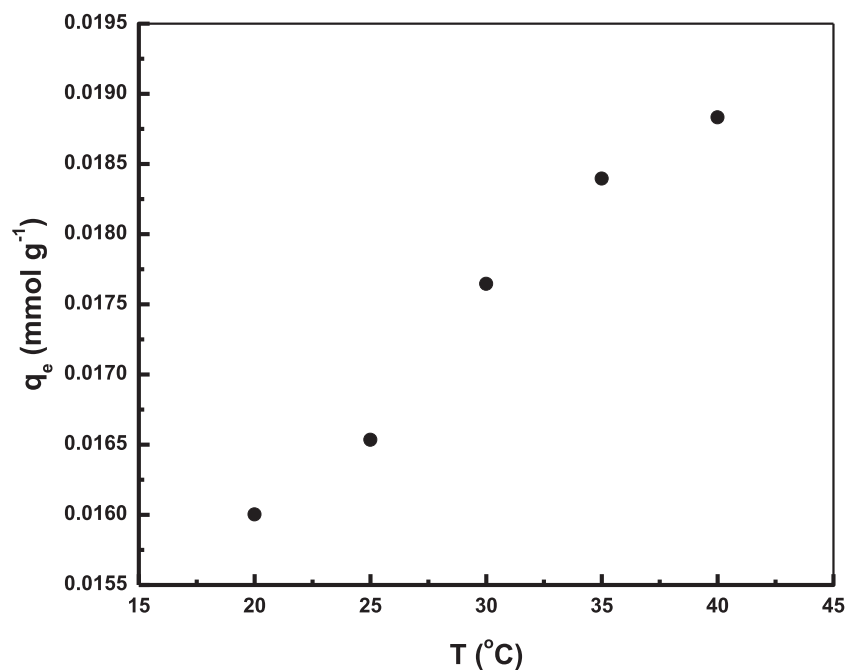


Fig. 9. Effect of temperature.

*Dubinin–Radushkevich isotherm*

The linear form of the Dubinin–Radushkevich isotherm^{31,32} is expressed as

$$(5) \quad \ln q_e = \ln Q_{DR} - K_{DR}\varepsilon^2$$

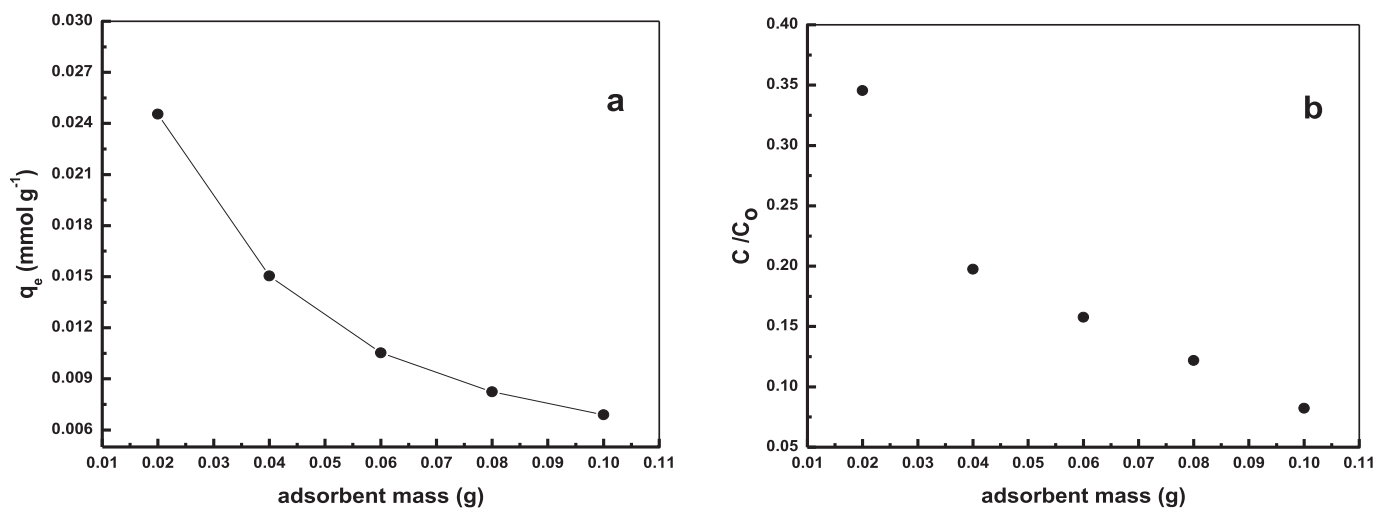
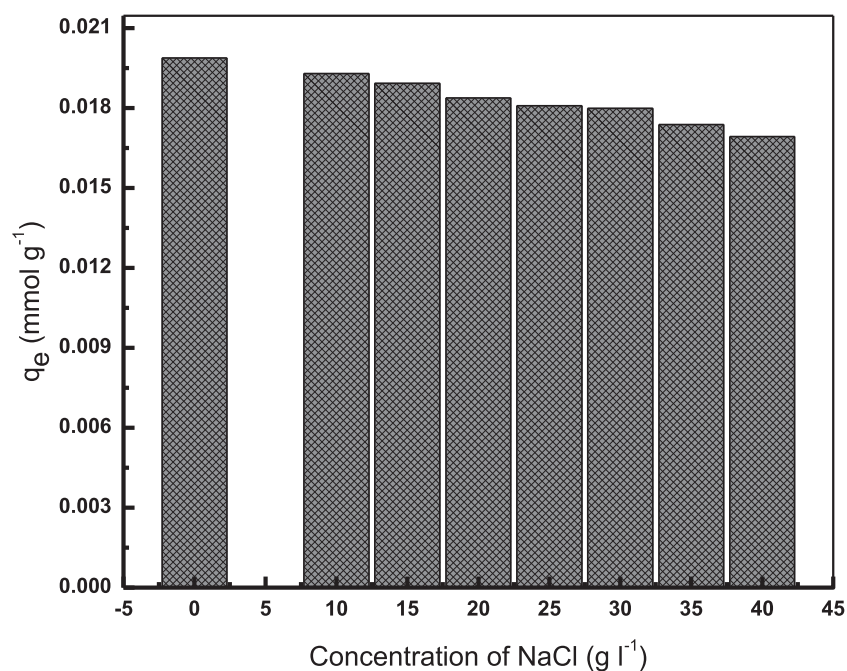
where q_e is the amount of the dye adsorbed per unit weight of the adsorbent (mg g^{-1}), Q_{DR} is the maximum sorption capacity provided by the intercept (mol g^{-1}), K_{DR} ($\text{mol}^2 \text{J}^{-2}$) is obtained from the slope of the straight-line plot of $\ln q_e$ versus ε^2 , and ε , the Polanyi potential, can be calculated as:

$$(6) \quad \varepsilon = RT \ln \left(1 + \frac{1}{C_e} \right)$$

where R is the universal gas constant ($\text{kJ mol}^{-1} \text{K}^{-1}$) and T is the temperature (Kelvin). E , the mean sorption energy, is calculated using the following relation:

$$(7) \quad E = \frac{1}{\sqrt{-2K_{DR}}}$$

Figure 13a presents $\ln q_e$ versus ε^2 plots for the RB5–TFCA at 25 °C. The value of E for RB5–TFCA was found to be less than

Fig. 10. Effect of sorbent dose on adsorption ($C_0 = 5 \times 10^{-4}$ mol/L; temperature = 25 ± 1 °C; pH 1).**Fig. 11.** Effect of ionic strength (addition of NaCl).

8 kJ mol⁻¹, suggesting that physisorption³³ is responsible for the adsorption process for both systems (Table 2).

Temkin isotherm

The Temkin isotherm assumes that the heat of adsorption of all the molecules increases linearly with coverage.³⁴ The linear form of this isotherm can be given as

$$(8) \quad q_e = \beta_T \ln K_T + \beta_T \ln C_e$$

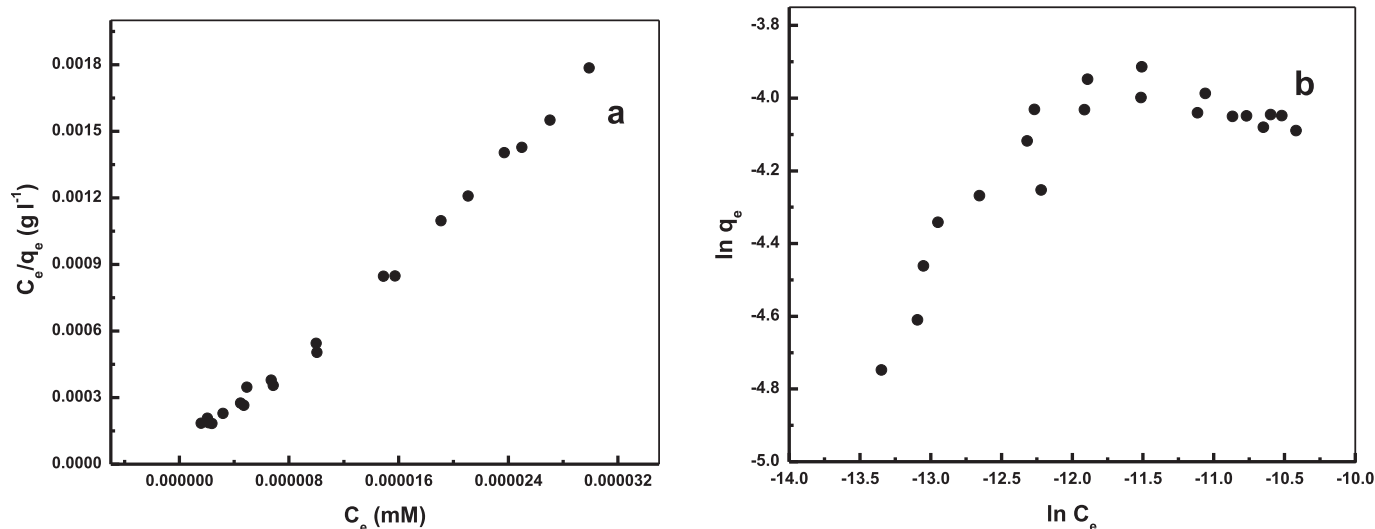
where q_e is the amount adsorbed at equilibrium (mmol g⁻¹), k_1 is the Temkin isotherm energy constant (L mol⁻¹), and k_2 is the Temkin isotherm constant. Plots between $\ln C_e$ versus q_e for TFCA (Fig. 13b) gave straight lines at 25 °C, thereby verifying the Temkin isotherm in the adsorption of RB5 over adsorbent. Slopes and intercepts of these straight lines that were helpful in determining the values of Temkin constants and these values are provided in Table 2 for TFCA.

Adsorption kinetic studies

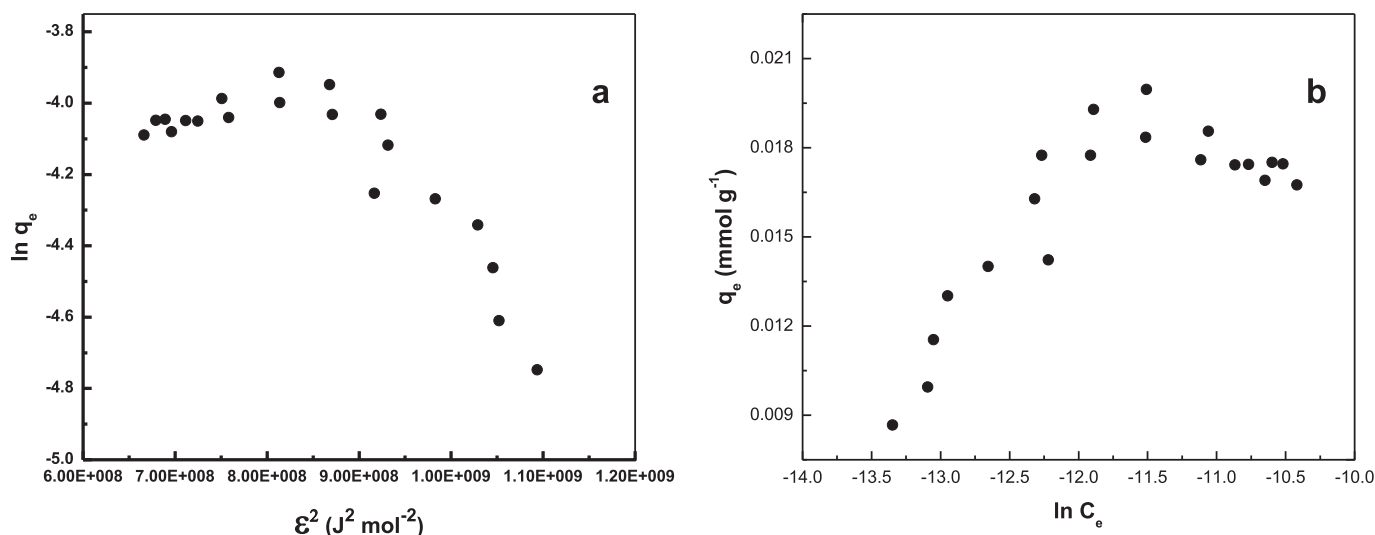
The study of adsorption kinetics describes the solute uptake rate and evidently this rate controls the residence time of adsorbate uptake at the solid-solution interface. The rate of removal of RB5 by adsorption was rapid initially and then slowed gradually until it attained an equilibrium beyond which there was significant increase in the rate of removal. The maximum adsorption of RB5 onto TFCA composite was observed at 90 min; therefore, this was fixed as the equilibrium time.

Aiming at evaluating the adsorption kinetics of RB5 onto TFCA composite, the pseudo first-order and pseudo second-order kinetic models were used to fit the experimental data, according to the below kinetic model equations. The pseudo first-order rate expression of Lagergren equation^{35,36} is given as

$$(9) \quad \log(q_e - q_t) = \log q_e - \left(\frac{K_1}{2.303}\right)t$$

Fig. 12. Adsorption isotherm models (a) Langmuir and (b) Freundlich for removal of RB5 on TFCA.**Table 2.** Adsorption isotherms, linear forms, and parameters of the sorption isotherm models.

Isotherm	Equation	Description	Value of parameters
Langmuir	$\frac{C_e}{q_e} = \frac{1}{q_m K_L} + \frac{C_e}{q_m}$	The constants q_m and K_L are calculated by the plot of C_e/q_e versus C_e with slope $1/q_m$ and intercept $1/(q_m K_L)$	$q_{m \text{ exp}}$ (mmole g^{-1}), 0.1875; q_m (mmol g^{-1}), 0.1992; K_L (L mg^{-1}); 90 438.78; R^2 , 0.995
Freundlich	$\ln q_e = \ln K_F + \frac{1}{n} \ln C_e$	K_F and $1/n$ can be calculated from a linear plot of $\ln q_e$ against $\ln C_e$	n , 2.6277; K_F (L mg^{-1}), 1.8525; R^2 , 0.8532
Dubinin–Radushkevich	$\ln q_e = \ln Q_{DR} - K_{DR} \varepsilon^2$	The slope of the plot of $\ln q_e$ versus ε^2 gives K_{DR} ($\text{mol}^2 (\text{kJ}^2)^{-1}$) and the intercept yields the adsorption capacity, Q_{DR} (mg g^{-1})	Q_{DR} , -0.1560; K_{DR} , -2.878×10^{-9} ; E_a , 2.011; R^2 , 0.8941
Temkin	$q_e = \beta_T \ln K_T + \beta_T \ln C_e$	The parameters B_T and K_T are the Temkin constants that can be determined by the plot of q_e versus $\ln C_e$	β_T , 71 051.68; K_T (L mg^{-1}), 14.3146; R^2 , 0.8611

Fig. 13. Adsorption isotherm models: (a) Dubinin–Radushkevich and (b) Temkin.

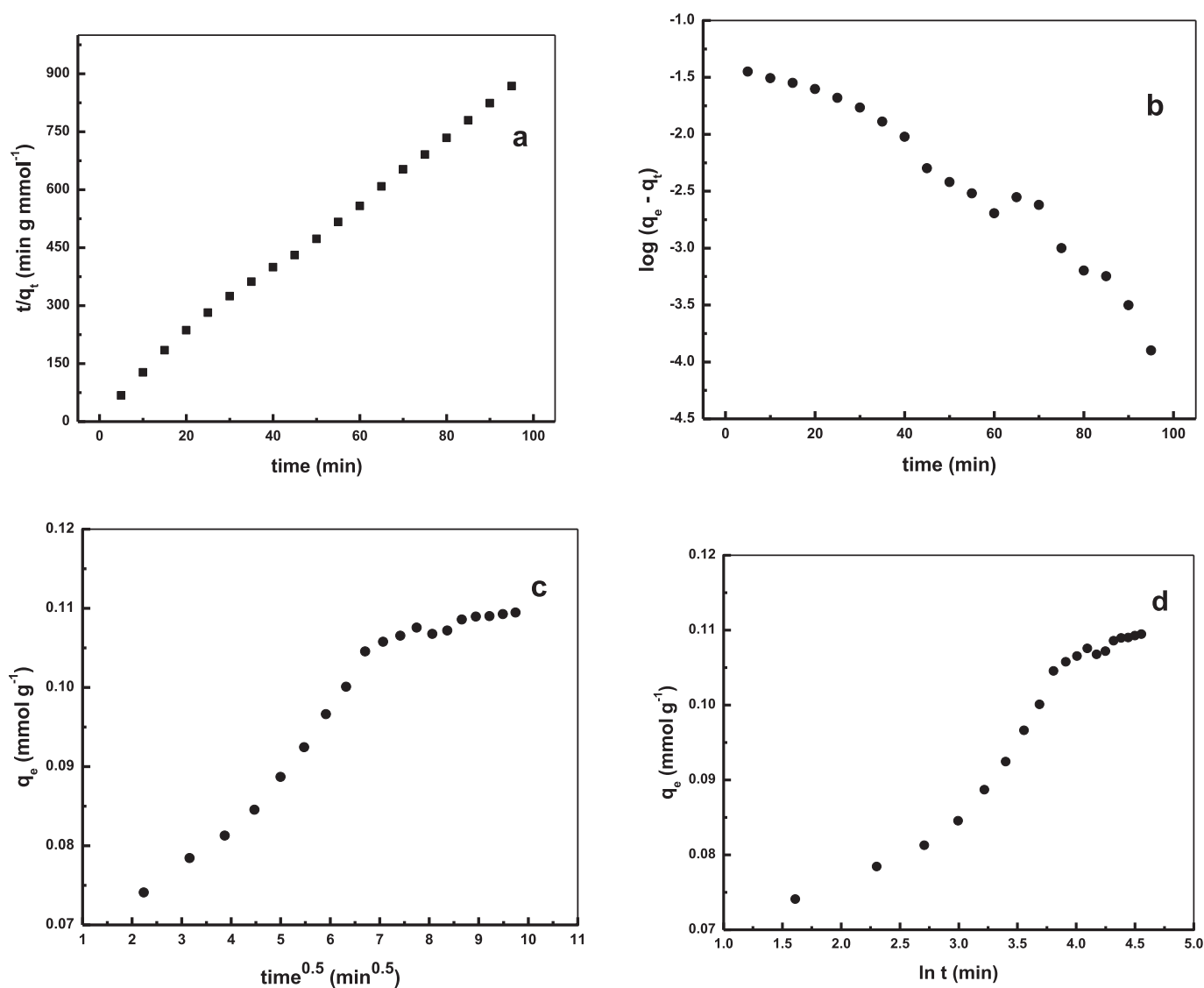
The pseudo second-order kinetic model³⁶ is expressed as

$$(10) \quad \frac{t}{q_t} = \frac{1}{K_2 q_e^2} + \left(\frac{1}{q_e}\right)t$$

where q_t is the amount of dye adsorbed (mmol g^{-1}) at various times t , q_e is the maximum adsorption capacity (mmol g^{-1}) for pseudo

first-order adsorption, k_1 is the pseudo first-order rate constant for the adsorption process (min^{-1}), q_t is the maximum adsorption capacity (mmol g^{-1}) for the pseudo second-order adsorption, k_2 is the rate constant of pseudo second-order adsorption ($\text{g mol}^{-1} \text{min}^{-1}$). The straight-line plots of $\log(q_e - q_t)$ versus t for the pseudo first-order reaction and t/q_t versus t for the pseudo second-order reaction (Figs. 14a and 14b) for adsorption of RB5 onto TFCA com-

F14

Fig. 14. Modeling of RB5 kinetic adsorption with TFCA: (a) PFORE, (b) PSORE, (c) intraparticle diffusion (Morris and Weber equation), and (d) Elovich.**Table 3.** Kinetic models, linear forms, and parameters for RB5 adsorption.

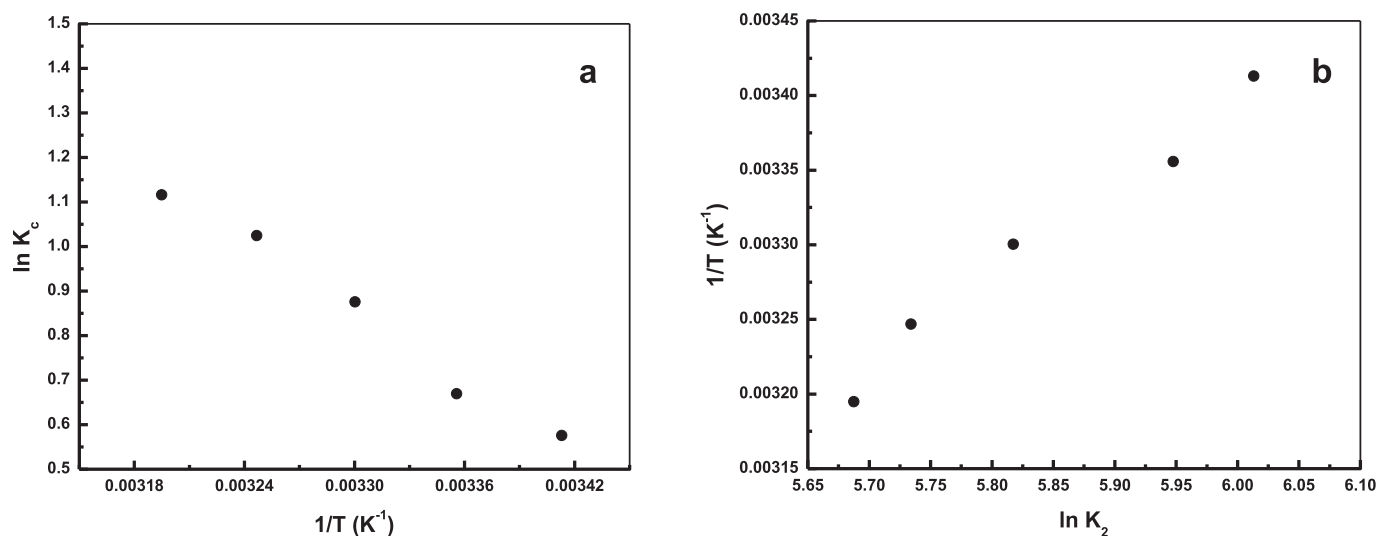
Model	Equation	Description	Value of parameters
Pseudo first-order kinetic	$\log(q_e - q_t) = \log q_e - \left(\frac{K_1}{2.303}\right)t$	The plot of $\ln(q_e - q_t)$ against t gives a straight line with the slope $-k_1$ and intercept $\ln q_e$	k_1 (min^{-1}), -0.0259 ; q_e (mmol g^{-1}), 0.3011 ; R^2 , 0.9079
Pseudo second-order kinetic	$\frac{t}{q_t} = \frac{1}{K_2 q_e^2} + \frac{t}{q_e}$	Values of k_2 and q_e for different initial concentrations of dye were calculated from the slope and intercept of the linear plot of t/q_t versus t	k_2 (min^{-1}), 12.9118 ; q_e (mmol g^{-1}), 1.97328 ; R^2 , 1
Intraparticle diffusion	$q_t = K_i t^{1/2} + X$	The parameters K_i and X were determined from the linear plot of q_t versus $t^{1/2}$	K_i ($\text{mg g}^{-1} \text{min}^{-1/2}$), 0.00109 ; X (mg g^{-1}), 1.9634 ; R^2 , 0.8595
Elovich	$q_t = \frac{1}{\beta} \ln(\alpha\beta) + \frac{1}{\beta} \ln t$	The constants α and β were obtained from the slope and intercept of a line plot of q_t versus $\ln t$	β (g mg^{-1}), 336.7 ; α ($\text{mg g}^{-1} \text{min}^{-1}$), 7.0979 ; R^2 , 0.9134
Experimental data	—	—	q_e (exp) (mmol g^{-1}), 1.9721

posite have also been tested to obtain the rate parameters. The k_1 , k_2 , q_e , q_t , and correlation coefficients, r_1^2 and r_2^2 for RB5 under different temperatures, were calculated from these plots and are given in Table 3. The correlation coefficient (r_1^2) for the pseudo first-order kinetic model is 0.9079 and the correlation coefficient (r_2^2) for the pseudo second-order kinetic model is 1.0. It is probable,

therefore, that this adsorption system is not a pseudo first-order reaction; rather, it fits the pseudo second-order kinetic model.

Thermodynamic parameters

In any adsorption process, both energy and entropy considerations must be considered to determine what process will occur

Fig. 15. (a) Van't Hoff and (b) Arrhenius plots for adsorption onto the adsorbent.**Table 4.** Standard enthalpy, entropy, and free energy changes for adsorption.

ΔH° (kJ mol ⁻¹)	ΔS° (J mol ⁻¹ K ⁻¹)	E_a (kJ mol ⁻¹)	ΔG° (kJ mol ⁻¹)				
			293 K	298 K	303 K	308 K	318 K
21.91	0.0794	5.13	-8.23	-9.11	-9.99	-10.88	-12.64

Table 5. Comparison of sorption capacity for RB5 dye with various adsorbents.

Adsorbent material	Initial pH	Contact time (min)	Temperature (°C)	Initial concentration (mg L ⁻¹)	Sorbent dosage (g L ⁻¹)	Sorption capacity (mg g ⁻¹)	Reference
Chitin	3.2	300	54	50	—	41.8	42
Nano-ZnO/CT-CB	4.0	360	30	30	0.1	198.44	43
Walnut wood activated carbon	5.0	120	30	40	0.6	19.34	44
Crosslinked chitosan	3.0	7200	30	4000	0.4	2941	45
Thiourea-formaldehyde alginate	1.0	60	25	0.03	0.02	198.36	This work

spontaneously. Values of thermodynamic parameters are the actual indicators for practical application of a process. The amount of RB5 adsorbed onto TFCA composite at equilibrium and at different temperatures (20, 25, 30, 40, and 45 °C) has been examined to obtain thermodynamic parameters for the adsorption system. The pseudo second order rate constant of RB5 adsorption is expressed as a function of temperature by the following Arrhenius-type relationship:³⁷

$$(11) \quad \ln K_2 = \ln A - \frac{E_a}{RT}$$

where E_a is the Arrhenius activation energy of adsorption, A is the Arrhenius factor, R is the gas constant and is equal to 8.314 J mol⁻¹ K⁻¹, and T is the operating temperature in Kelvin. A linear plot of $\ln k_2$ vs $1/T$ for the adsorption of RB5 onto TFCA composite (Fig. 15a) was constructed to generate the activation energy from the slope ($-E_a/R$). The chemical (chemisorption) or physical (physisorption) adsorption mechanism is often an important indicator to describe the type of interactions between RB5 and TFCA composite. The magnitude of activation energy gives an idea of the type of adsorption, which is mainly physical or chemical. Low activation energies (5–40 kJ mol⁻¹) are characteristic for physisorption, whereas higher activation energies (40–800 kJ mol⁻¹) suggest chemisorption.³⁸ The result obtained is +5.13 kJ mol⁻¹ (Table 4) for the adsorption of RB5 onto TFCA composite, indicating that the adsorption has a low potential barrier and corresponds to physisorption. The other thermodynamic parameters,

change in the standard free energy (ΔG°), enthalpy (ΔH°), and entropy (ΔS°), were determined by using following equations:

$$(12) \quad K_c = \frac{C_e}{C_s}$$

$$(13) \quad \Delta G^\circ = -RT \ln K_c$$

$$(14) \quad \ln K_c = \frac{\Delta S^\circ}{R} - \frac{\Delta H^\circ}{RT}$$

where K_c is the equilibrium constant, C_e is the amount of RB5 adsorbed on the TFCA composite of the solution at equilibrium (mol L⁻¹), C_s is the equilibrium concentration of the RB5 in the solution (mol L⁻¹). The K_2 of the pseudo second-order model was used to obtain C_e and C_s , T is the solution temperature (Kelvin), and R is the gas constant. ΔH° and ΔS° were calculated from the slope and the intercept of van't Hoff plots of $\ln K_c$ vs $1/T$ (Fig. 15b), and the values of adsorption thermodynamic parameters are listed in Table 4. The negative value of the change of free energy (ΔG°) (-8.23, -9.11, -9.99, -10.88, and -12.64) confirms the feasibility of the adsorption process and also indicates spontaneous adsorption of RB5 onto TFCA composite in the temperature range studied.³⁹ The positive value of the standard enthalpy change (ΔH°) (21.91 kJ mol⁻¹) indicates that the adsorption is physical in nature involving weak forces of attraction and is also endothermic.

mic, thereby demonstrating that the process is stable energetically. At the same time, the low value of ΔH° implies that there was loose bonding between the adsorbate molecules and the adsorbent surface. The positive value of standard entropy change (ΔS°) ($0.0794 \text{ J mol}^{-1} \text{ K}^{-1}$) suggests the increased randomness at the solid-solution interface during the adsorption of RB5 onto TFCA composite.

The diagram obtained in Langmuir plots further helps in the determination of thermodynamic parameters. Gibb's free energy (ΔG°), change in entropy (ΔS°), and change in enthalpy (ΔH°) were calculated using the following relations:⁴⁰

$$(15) \quad \Delta G^\circ = -RT \ln K_c$$

$$(16) \quad \Delta H^\circ = -R \left(\frac{T_2 T_1}{T_2 - T_1} \right) \ln \left(\frac{K_{c2}}{K_{c1}} \right)$$

$$(17) \quad \Delta G^\circ = \Delta H^\circ - T \Delta S^\circ$$

where K_c , K_{c1} , and K_{c2} are the Langmuir constants at 20, 30, and 40 °C, respectively, as obtained from slopes and intercepts of Langmuir isotherms. The positive values of entropy change and enthalpy show the increased randomness and endothermic nature of the process, respectively, whereas the negative values of free energy suggest the feasibility of the process. The above values have been calculated for both adsorption systems and are presented in Table 4.

Desorption studies

Desorption studies help to elucidate the mechanism and recovery of the adsorbate and adsorbent. TFCA composite was washed three times with sodium hydroxide solution at a pH around 12, filtered, left to dry at 50 °C in an oven overnight, and stored on a desiccator prior to reuse in the adsorption again. As the pH of desorbing solution increased, the percentage of desorption increased. As the pH of the system increased, the number of negatively charged sites increased. A negatively charged site on the adsorbent favors the desorption of dye anions due to the electrostatic repulsion.⁴¹ At pH 12, a significantly high electrostatic repulsion exists between the negatively charged surface of the adsorbent and anionic dye. The removal of dye by adsorption on the adsorbent (TFCA) was compared before and after the recovery process under the same conditions: initial concentration of dye solution, $3 \times 10^{-5} \text{ mol/L}$, temperature of approximately 25 °C, pH 1, and 0.02 g adsorbent dosage for 60 min. The maximum adsorption of RB5 dye onto TFCA composite before the recovery process was 88.10%, whereas after the recovery process, it was 87.50%.

Comparison of adsorption of RB5 dye with various sorbents

Table 5 shows the comparison of maximum sorption capacities of the TFCA with a series of values found in the literature (together with the best operating conditions reported by respective authors). The TFCA adsorbent has a adsorption capacity of the same order of magnitude as other sorbents; although the utilization of chitin adsorbent,⁴² nano-ZnO/Chitosan composite beads (nano-ZnO/CT-CB),⁴³ the potential of using walnut wood activated carbon as low-cost adsorbents,⁴⁴ and the templated crosslinked-chitosan microparticles⁴⁵ showed better adsorption capacity. It is noteworthy that the TFCA sorbent has an important advantage related to their fast kinetics. The high sorption capacity of the TFCA adsorbents towards RB5 dye reveals that adsorbent could be promising for practical application in RB5 dye removal from wastewater.

Conclusion

The present study clearly demonstrated that TFCA can be very effectively employed for the removal of dyestuff RB5 from aque-

ous solution and wastewaters. These materials are available freely, locally, and have been proven to be much more efficient than the conventional expensive adsorbents. The preliminary adsorption data were obtained by observing the effect of pH, concentration, contact time, temperature, dose of adsorbent, etc., and their dependence on adsorption was determined. The high adsorption capacity of RB5 onto TFCA composite in highly acidic solutions (pH 1) is due to the strong electrostatic interactions between its adsorption site and dye anion. Adsorption isotherm parameters for Langmuir, Freundlich, D-R, and Temkin were determined and their constants were calculated. The equilibrium data fit well the Freundlich model of adsorption for RB5 dye. The highest value of n at equilibrium (2.62) suggests that the adsorption is physical. The kinetic data tends to fit very well in the pseudo second-order kinetic model with high correlation coefficients, and the adsorption process is interpreted as film diffusion at all temperatures. The negative values of ΔG° indicate the spontaneity of the process, and the negative value of ΔH° reveals that the adsorption process was exothermic in nature and a physical adsorption. The positive value of ΔS° implies the increment of an orderliness between the adsorbate and the adsorbent molecules. SEM images show well-defined and characterized morphological images that are evidence for the effective adsorption of RB5 molecules on the cavities and pores of the TFCA composite. Desorption studies were conducted and the results showed that TFCA composite can be used in adsorption of acid dyes several times by regeneration process using sodium hydroxide solution at a pH around 12.

References

- Xie, Y. J.; Yan, B.; Xu, H. L.; Chen, J.; Liu, Q. X.; Deng, Y. H.; Zeng, H. B. *ACS Appl. Mater. Interfaces* **2014**, *6*, 8845. doi:10.1021/am501632f.
- Yan, H.; Li, H. J.; Tao, X.; Li, K.; Yang, H.; Li, A. M.; Xiao, S. J.; Cheng, R. S. *ACS Appl. Mater. Interfaces* **2014**, *6*, 9871. doi:10.1021/am502377n.
- Unuabonah, E. I.; Günter, C.; Weber, J.; Lubahn, S.; Taubert, A. *ACS Sustainable Chem. Eng.* **2013**, *1*, 966. doi:10.1021/sc400051y.
- Amaral, F. M.; Kato, M. T.; Florêncio, L.; Gavazza, S. *Bioresour. Technol.* **2014**, *163*, 364. doi:10.1016/j.biortech.2014.04.026.
- Bakheet, B.; Yuan, S.; Li, Z.; Wang, H.; Zuo, J.; Komarneni, S.; Wang, Y. *Water Res.* **2013**, *47*, 6234. doi:10.1016/j.watres.2013.07.042.
- Zhang, S. X.; Zhang, Y. Y.; Bi, G. M.; Liu, J. S.; Wang, Z. G.; Xu, Q.; Xu, H.; Li, X. Y. *J. Hazard. Mater.* **2014**, *270*, 27. doi:10.1016/j.jhazmat.2014.01.039.
- Mathieu-Denoncourt, J.; Martyniuk, C. J.; de Solla, S. R.; Balakrishnan, V. K.; Langlois, V. S. *Environ. Sci. Technol.* **2014**, *48*, 2952. doi:10.1021/es500263x.
- de Luna, L. A.; da Silva, T. H.; Nogueira, R. F.; Kummrow, F.; Umbuzeiro, G. A. *J. Hazard. Mater.* **2014**, *276*, 332. doi:10.1016/j.jhazmat.2014.05.047.
- Gunatilake, S. K. *J. Multidiscip. Eng. Sci. Stud.* **2015**, *1* (1), 12.
- Verma, A. K.; Dash, R. R.; Bhunia, P. *J. Environ. Manage.* **2012**, *93*, 154. doi:10.1016/j.jenvman.2011.09.012.
- Gezer, N.; Gülfen, M.; Aydın, A. O. *J. Appl. Polym. Sci.* **2011**, *122*, 1134. doi:10.1002/app.34246.
- Tan, W. S.; Ting, A. S. Y. *Bioresour. Technol.* **2014**, *160*, 115. doi:10.1016/j.biortech.2013.12.056.
- Daemi, H.; Barikani, M.; Barmar, M. *Carbohydr. Polym.* **2013**, *92*, 490. doi:10.1016/j.carbpol.2012.09.046.
- Birinci, E.; Gülfen, M.; Aydın, A. O. *Hydrometallurgy* **2009**, *95*, 15. doi:10.1016/j.hydromet.2008.04.002.
- Zhou, Y. T.; Nie, H. L.; Branford-White, C.; He, Z. Y.; Zhu, L. M. *J. Colloid Interface Sci.* **2009**, *330*, 29. doi:10.1016/j.jcis.2008.10.026.
- Li, G. Y.; Jiang, Y. R.; Huang, K. L.; Ding, P.; Chen, J. J. *Alloys Compd.* **2008**, *466*, 451. doi:10.1016/j.jallcom.2007.11.100.
- El-Korashy, S. A.; Elwakeel, K. Z.; El-Hafeiz, A. A. *J. Cleaner Prod.* **2016**, *137*, 40. doi:10.1016/j.jclepro.2016.07.073.
- Chen, B.; Yang, Z.; Ma, G.; Kong, D.; Xiong, W.; Wang, J.; Zhu, Y.; Xia, Y. *Microporous Mesoporous Mater.* **2018**, *257*, 1. doi:10.1016/j.micromeso.2017.08.026.
- Ai, L.; Zhang, C.; Liao, F.; Wang, Y.; Li, M.; Meng, L.; Jiang, J. *J. Hazard. Mater.* **2011**, *198*, 282. doi:10.1016/j.jhazmat.2011.10.041.
- El-Bindary, A. A.; Diab, M. A.; Hussien, M. A.; El-Sonbati, A. Z.; Eessa, A. M. *Spectrochim. Acta, Part A* **2014**, *124*, 70. doi:10.1016/j.saa.2013.12.109.
- Banerjee, S.; Chattopadhyaya, M. C. *Arab. J. Chem.* **2017**, *10*, S1629. doi:10.1016/j.arabj.2013.06.005.
- Elwakeel, K. Z.; El-Bindary, A. A.; El-Sonbati, A. Z.; Hawas, A. R. *Can. J. Chem.* **2017**, *95*, 807. doi:10.1139/cjc-2016-0641.

- (23) Elwakeel, K. Z.; Guibal, E. *Chem. Eng. J.* **2015**, *281*, 345. doi:10.1016/j.cej.2015.05.110.
- (24) Ahmad, R.; Kumar, R. J. *Environ. Manage.* **2010**, *91*, 1032. doi:10.1016/j.jenvman.2009.12.016.
- (25) El-Halwany, M. M. *Desalination* **2010**, *250*, 208. doi:10.1016/j.desal.2008.07.030.
- (26) Foo, K. Y.; Hameed, B. H. *Chem. Eng. J.* **2010**, *156*, 2. doi:10.1016/j.cej.2009.09.013.
- (27) Yadav, D. *Int. J. Res. Chem. Environ.* **2016**, *6* (3), 7.
- (28) Mittal, A.; Mittal, J.; Malviya, A.; Kaur, D.; Gupta, V. K. J. *Colloid Interface Sci.* **2010**, *343*, 463. doi:10.1016/j.jcis.2009.11.060.
- (29) Selvam, P. P.; Preethi, S.; Basakaralingam, P.; Thinakaran, N.; Sivasamy, A.; Sivanesan, S. J. *Hazard. Mater.* **2008**, *155*, 39. doi:10.1016/j.jhazmat.2007.11.025.
- (30) Özcan, A. S.; Erdem, B.; Özcan, A. *Colloids Surf., A* **2005**, *266*, 73. doi:10.1016/j.colsurfa.2005.06.001.
- (31) Karim, A. B.; Mounir, B.; Hachkar, M.; Bakasse, M.; Yaacoubi, A. J. *Hazard. Mater.* **2009**, *168*, 304. doi:10.1016/j.jhazmat.2009.02.028.
- (32) Seki, Y.; Yurdakoç, K. *Colloids Surf., A* **2009**, *340*, 143. doi:10.1016/j.colsurfa.2009.03.020.
- (33) Chowdhury, S.; Mishra, R.; Saha, P.; Kushwaha, P. *Desalination* **2011**, *265*, 159. doi:10.1016/j.desal.2010.07.047.
- (34) Senthil Kumar, P.; Ramalingam, S.; Senthamarai, C.; Niranjanaa, M.; Vijayalakshmi, P.; Sivanesan, S. *Desalination* **2010**, *261*, 52. doi:10.1016/j.desal.2010.05.032.
- (35) Ono, Y.; Amano, Y.; Aikawa, M.; Machida, M. *Kagaku Kogaku Ronbunshu* **2011**, *37*, 22. doi:10.1252/kakoronbunshu.37.22.
- (36) Goel, N. K.; Kumar, V.; Pahan, S.; Bhardwaj, Y. K.; Sabharwal, S. J. *Hazard. Mater.* **2011**, *193*, 17. doi:10.1016/j.jhazmat.2011.05.026.
- (37) Baral, S. S.; Das, S. N.; Rath, P. *Biochem. Eng. J.* **2006**, *31*, 216. doi:10.1016/j.bej.2006.08.003.
- (38) Doğan, M.; Abak, H.; Alkan, M. J. *Hazard. Mater.* **2009**, *164*, 172. doi:10.1016/j.jhazmat.2008.07.155.
- (39) Hong, S.; Wen, C.; He, J.; Gan, F.; Ho, Y. S. J. *Hazard. Mater.* **2009**, *167*, 630. doi:10.1016/j.jhazmat.2009.01.014.
- (40) Lakshmi, U. R.; Srivastava, V. C.; Mall, I. D.; Lataye, D. H. J. *Environ. Manage.* **2009**, *90*, 710. doi:10.1016/j.jenvman.2008.01.002.
- (41) Mahmoodi, N. M.; Hayati, B.; Arami, M.; Lan, C. *Desalination* **2011**, *268*, 117. doi:10.1016/j.desal.2010.10.007.
- (42) Begum, H. A.; Mondal, A. K.; Muslim, T. *Bangladesh Pharm. J.* **2012**, *15*, 145. doi:10.3329/bpj.v15i2.12580.
- (43) Çınar, S.; Kaynar, Ü. H.; Aydemir, T.; Çam Kaynar, S.; Ayvaci, M. *Int. J. Biol. Macromol.* **2017**, *96*, 459. doi:10.1016/j.ijbiomac.2016.12.021.
- (44) Heibati, B.; Rodriguez-Couto, S.; Amrane, A.; Rafatullah, M.; Hawari, A.; Al-Ghouti, M. A. J. *Ind. Eng. Chem.* **2014**, *20*, 2939. doi:10.1016/j.jiec.2013.10.063.
- (45) Chen, A. H.; Huang, Y. Y. J. *Hazard. Mater.* **2010**, *177*, 668. doi:10.1016/j.jhazmat.2009.12.083.